Supplementary Information: Fossil corals with various degrees of preservation can retain information about biomineralization-related organic material

Jeana L. Drake[1,2,3*+], Maxence Guillermic[2,4,5+], Robert A. Eagle[2,4,5], David K. Jacobs[2,3*]

[1]Department of Marine Biology, University of Haifa, Israel

[2]Department of Earth, Planetary, and Space Sciences, University of California – Los Angeles, 595 Charles Young Drive E., Los Angeles, CA 90095, USA

[3]Department of Ecology and Evolutionary Biology, University of California – Los Angeles, 612 Charles Young Drive E., Los Angeles, CA 90095, USA

[4]Department of Atmospheric and Oceanic Sciences, Institute of the Environment and Sustainability, 520 Portola Plaza, University of California – Los Angeles, CA 90095, USA

[5]Université de Brest Occidentale, Institut Universitaire Européen de la Mer, LGO, Rue Dumont d'Urville, 29280, Plouzané, France

[+]These authors have contributed equally to this work and share first authorship.

1 Elemental measurement reproducibility and uncertainty

The typical blanks for a 30 ppm Ca session were: $^{7}Li < 2\%$, $^{11}B < 7\%$, $^{25}Mg < 0.2\%$ and $^{43}Ca < 0.02\%$. Analytical uncertainty of a single measurement was calculated from the reproducibility of the Cam-Wuellestorfi, measured during a particular mass spectrometry session. The analytical uncertainties on the X/Ca ratios are: ±7 µmol/mol for B/Ca, ±0.01 mmol/mol for Sr/Ca, ±0.01 mmol/mol for Mg/Ca, ±0.4 µmol/mol for Li/Ca, ±0.1 µmol/mol for Ba/Ca, and ±7 µmol/mol for Mn/Ca, respectively (Guillermic et al., 2020).

2 Range of elemental ratios from modern corals

We did not attempt to make an exhaustive compilation of modern element/Ca ratios. The ranges presented for B/Ca, Sr/Ca, Mg/Ca, Li/Ca, Ba/Ca and Mn/Ca grey bars in Fig. 1 and 3 are presented at 2 SD.

B/Ca modern range was calculated based on 336 values from 6 corals, B/Ca = 483 +/- 200 µmol/mol (2 SD, n= 336, (Comeau et al., 2017;McCulloch et al., 2017;Guillermic et al., accepted)).

Sr/Ca modern range was calculated based on 1722 values from 9 corals, Sr/Ca = 9.1 +/- 0.4 mmol/mol (2 SD, n=1722, (Felis et al., 2004;Kuhnert et al., 2005;Allison et al., 2011;Giry et al., 2012;D'Olivo et al., 2019;Guillermic et al., accepted)).

Mg/Ca modern range was calculated based on 699 values from 7 corals, Mg/Ca = 4.8 +/- 1.1 mmol/mol (2 SD, n=699, Felis et al., 2014a; (Allison et al., 2011;Hathorne et al., 2013b;D'Olivo et al., 2019;Guillermic et al., accepted)).

Li/Ca modern range was calculated based on 690 values from 5 corals, Li/Ca = 6.6 +/- 1.2 µmol/mol (2SD, n=690, (Hathorne et al., 2013a;D'Olivo et al., 2019;Guillermic et al., accepted)).

Ba/Ca modern range was calculated based on 82 values from 2 corals, Ba/Ca=29 +/- 23 µmol/mol (2SD, n=82, (Guillermic et al., accepted)).

Mn/Ca modern range was selected between 0.01–10 µmol/mol (Shen et al., 1991).

3 Supplementary Figures

Supplementary Figure 1. X-ray powder diffractogram for ground and cleaned powders of select fossil specimens examined here. As milling can lead to recrystallization of aragonite to calcite (Gill et al., 1995;Waite and Swart), we chose to examine bulk ground powders of three specimens displaying mixed mineralogies of milled powders whose values are averaged between sub-samples taken within versus between corallites. This further analysis revealed that *P. maigensis* was 90/10 (previously 96.5/3.5), *M. annularis* 6 was 75/25 (previously 85/15), and *O. cavernosa* was 93/7 (previously 86.5/13.5) aragonite/calcite. This reveals no significant effect between the grinding/milling sample preparation in this study.

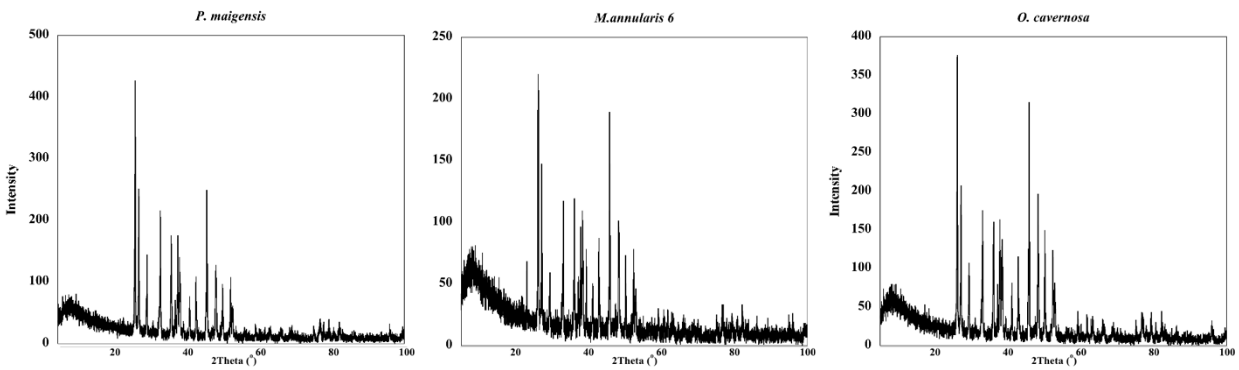

Supplementary Figure 2. X-ray power diffractogram for milled and cleaned powders of modern and fossil specimens examined here, arranged from 100% aragonite to 100% calcite/silicified. Species names used here are those provided by the loaning museum. Instrument and software settings were to analyze each sample from 5 to 100^0 2θ for 10 s/step on 0.0167° steps at 45 kV and 40 mA, with irradiance length set to 10 mm of continuous width, a 1° fixed antiscatter slit applied to the incident beam, and 0.04 rad sollar slits applied to incident and diffracted beams. The modern *O. annularis* and fossils *O. annularis* 3 and 4 as well as *M. cavernosa* 1 have previously been reported in (Drake et al., 2020) and are reproduced with modifications here with permission of the journal of their original publication.

Pocillopora damicornis (modern)

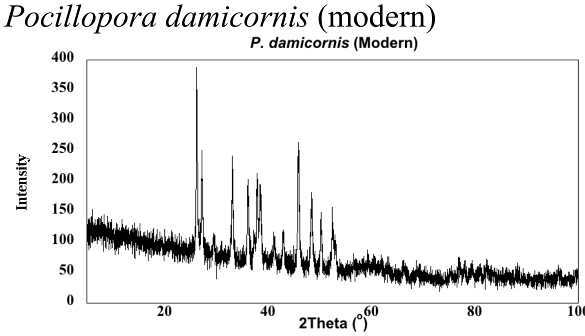

Orbicella annularis (modern)

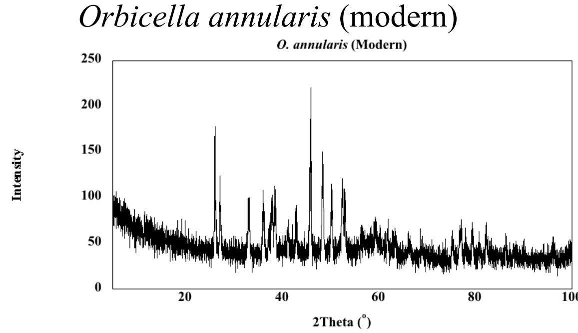

Porites californica

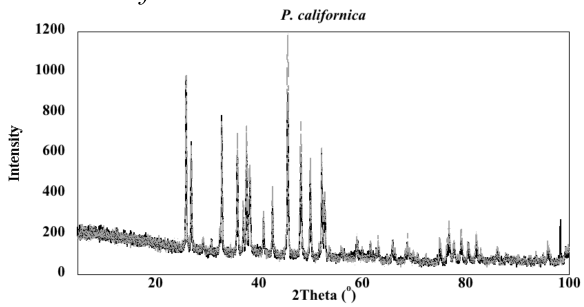

Montastraea annularis 3

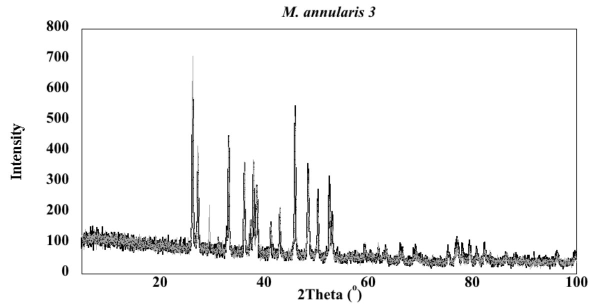

Orbicella limbata

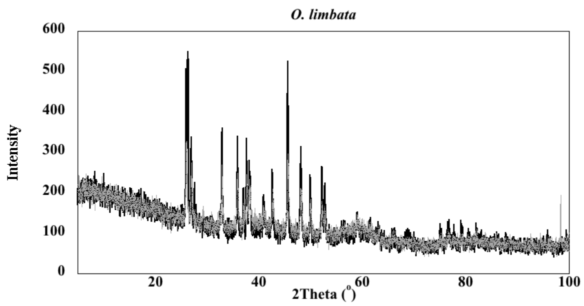

Porites clavaria

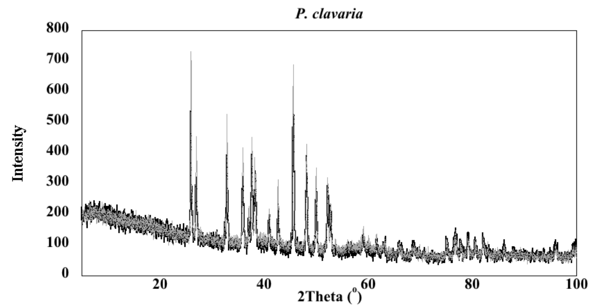

Stylophora affinis

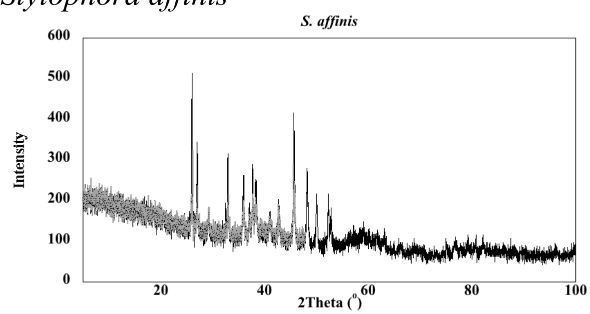

Porites maigensis

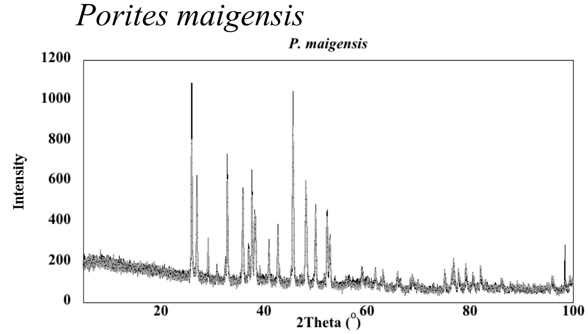

Montastraea annularis 4

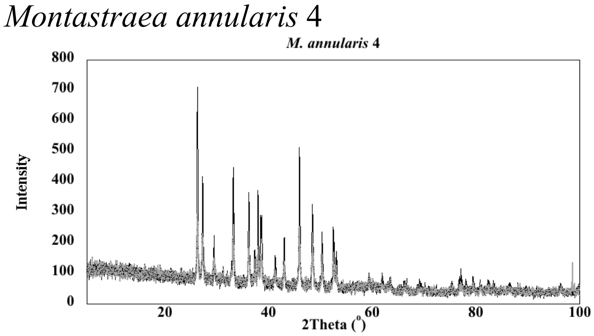

Orbicella cavernosa

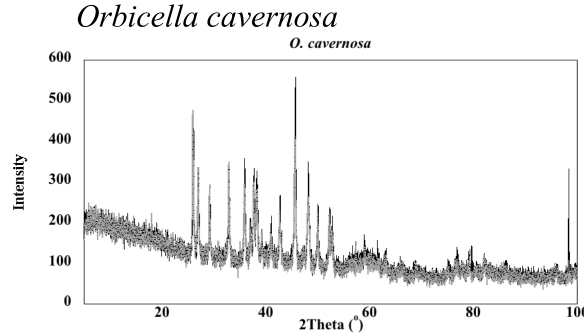

Porites sp.

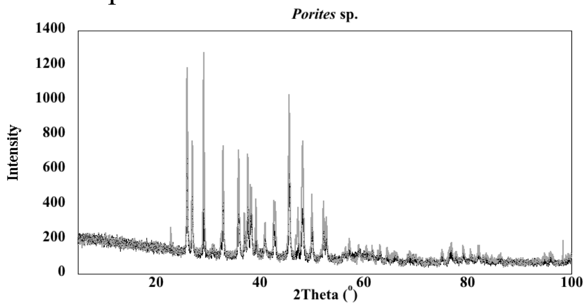

Montastraea annularis 6

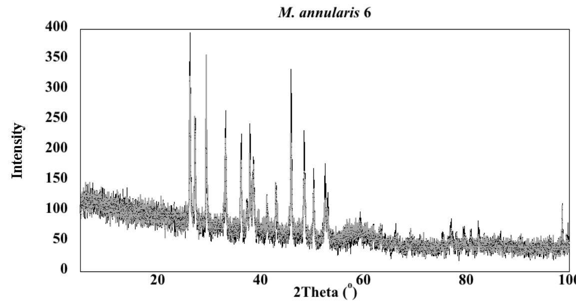

Montastraea cavernosa 1

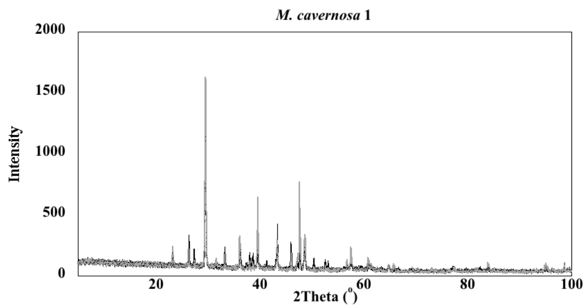

Favia distans

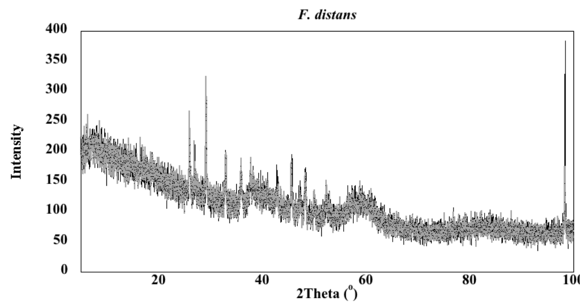

Stylophora conferta

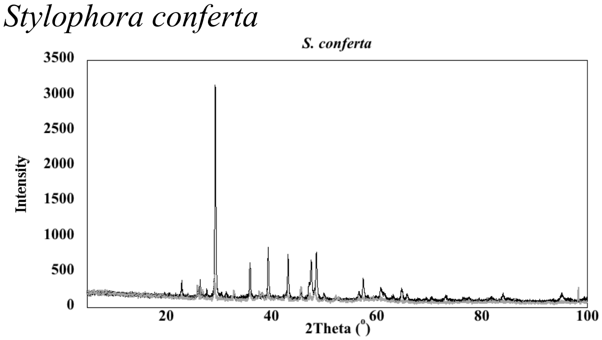

Montastraea annularis 2

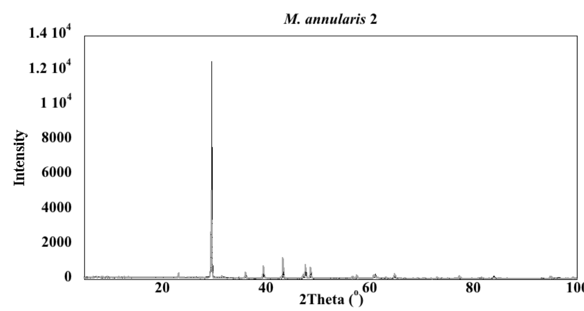

Favia sp. 1

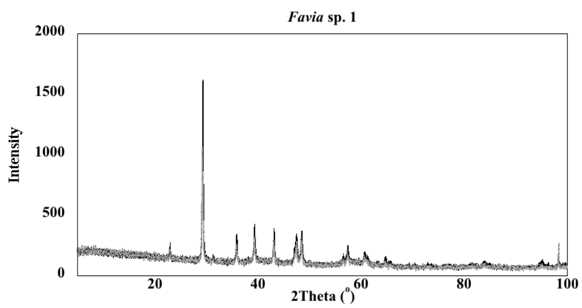

Favia sp. 2

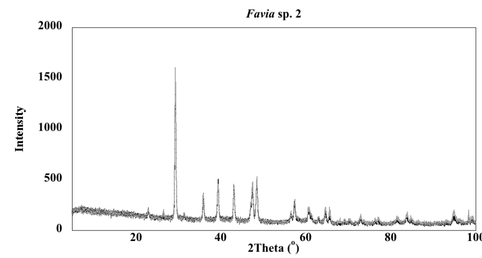

Zaphrentis dalli

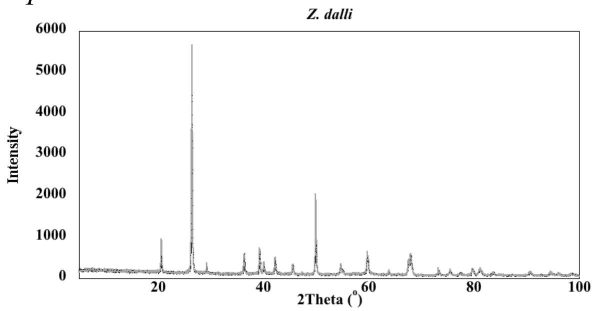

Supplementary Figure 3. Scanning electron micrographs of three Pleistocene corals displaying a range of mineralogies. *M. annularis* 4 is >90% aragonite (a,d,g), *M. annularis* 6 is 85/15 aragonite/calcite (b,e,h), and *M. annuarlis* 2 is >90% calcite (c,f,i). A change of texture is observed from the >90% aragonite sample (a, d, g) to the >90% calcite sample (c, f, i) which exhibits a blocky texture.

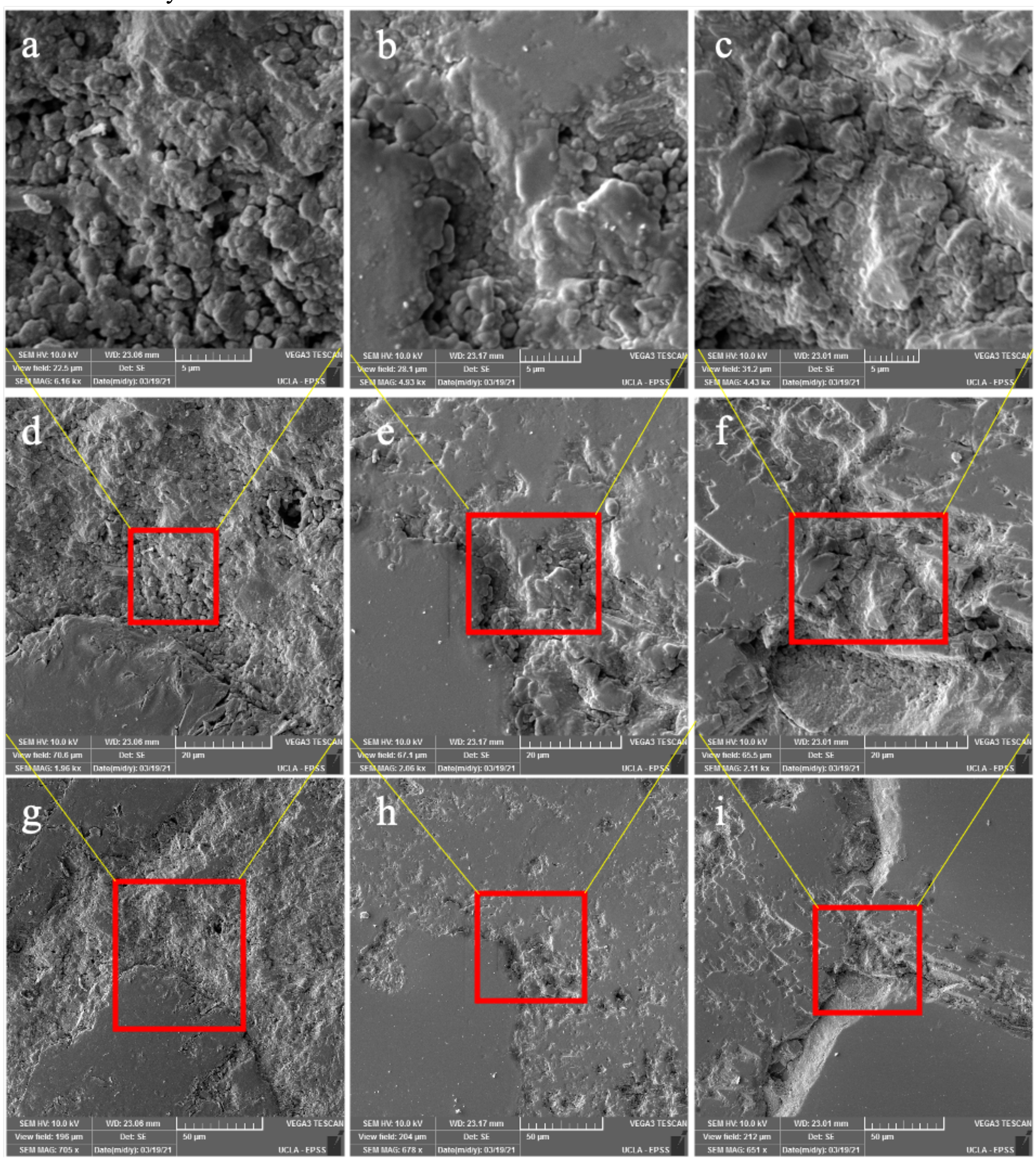

4 Supplementary Table Legends

Supplementary Table 1. Trace elements of fossil coral skeletons displaying a range of mineralogies.

Supplementary Table 2. Racemization and composition of amino acids extracted as free and/or peptide-bound from modern and fossil coral skeletons.

Supplementary Table 3. Results of Wilcoxon tests comparing amino acid composition of grouped modern and fossil coral skeletons.

5 References

Allison, N., Cohen, I., Finch, A.A., and Erez, J. (2011). Controls on Sr/Ca and Mg/Ca in scleractinian corals: The effects of Ca-ATPase and transcellular Ca channels on skeletal chemistry. *Geochimica et Cosmochimica Acta* 75**,** 6350-6360.

Comeau, S., Cornwall, C., and McCulloch, M. (2017). Decoupling between the response of coral calcifying fluid pH and calcification to ocean acidification. *Scientific Reports* 7**,** 1-10.

D'Olivo, J.P., Georgiou, L., Falter, J., DeCarlo, T.M., Irigoien, X., Voolstra, C.R., Roder, C., Trotter, J., and McCulloch, M.T. (2019). Long-term impacts of the 1997–1998 bleaching event on the growth and resilience of massive Porites corals from the central Red Sea. *Geochemistry, Geophysics, Geosystems* 20**,** 2936-2954.

Drake, J.L., Whitelegge, J.P., and Jacobs, D.K. (2020). First sequencing of ancient coral skeletal proteins. *Scientific Reports* 10**,** 1-11.

Felis, T., Lohmann, G., Kuhnert, H., Lorenz, S.J., Scholz, D., Pätzold, J., Al-Rousan, S.A., and Al-Moghrabi, S.M. (2004). Increased seasonality in Middle East temperatures during the last interglacial period. *Nature* 429**,** 164-168.

Gill, I., Olson, J.J., and Hubbard, D.K. (1995). Corals, paleotemperature records, and the aragonite-calcite transformation. *Geology* 23**,** 333-336.

Giry, C., Felis, T., Kölling, M., Scholz, D., Wei, W., Lohmann, G., and Scheffers, S. (2012). Mid-to late Holocene changes in tropical Atlantic temperature seasonality and interannual to multidecadal variability documented in southern Caribbean corals. *Earth and Planetary Science Letters* 331**,** 187-200.

Guillermic, M., L., C.P., De Corte, I., Misra, S., Bijma, J., de Beer, D., Reymond, C., Westphal, H., Ries, J., and Eagle, R. (accepted). Thermal stress reduces Pocilloporid coral resilience to ocean acidification by impairing control over calcifying fluid chemistry. *Science Advances*.

Guillermic, M., Misra, S., Eagle, R., Villa, A., Chang, F., and Tripati, A. (2020). Seawater pH reconstruction using boron isotopes in multiple planktonic foraminifera species with different depth habitats and their potential to constrain pH and pCO_2 gradients. *Biogeosciences* 17**,** 3487-3510.

Hathorne, E.C., Felis, T., Suzuki, A., Kawahata, H., and Cabioch, G. (2013a). Lithium in the aragonite skeletons of massive Porites corals: A new tool to reconstruct tropical sea surface temperatures. *Paleoceanography* 28**,** 143-152.

Hathorne, E.C., Gagnon, A., Felis, T., Adkins, J., Asami, R., Boer, W., Caillon, N., Case, D., Cobb, K.M., and Douville, E. (2013b). Interlaboratory study for coral Sr/Ca and other element/Ca ratio measurements. *Geochemistry, Geophysics, Geosystems* 14**,** 3730-3750.

Kuhnert, H., Crüger, T., and Pätzold, J. (2005). NAO signature in a Bermuda coral Sr/Ca record. *Geochemistry, Geophysics, Geosystems* 6.

McCulloch, M.T., D'Olivo, J.P., Falter, J., Holcomb, M., and Trotter, J.A. (2017). Coral calcification in a changing world and the interactive dynamics of pH and DIC upregulation. *Nature communications* 8**,** 15686.

Shen, G.T., Campbell, T.M., Dunbar, R.B., Wellington, G.M., Colgan, M.W., and Glynn, P.W. (1991). Paleochemistry of manganese in corals from the Galapagos Islands. *Coral Reefs* 10**,** 91-100.

Waite, A.J., and Swart, P.K. (2015). The inversion of aragonite to calcite during the sampling of skeletal archives: implications for proxy interpretation. *Rapid Communications in Mass Spectrometry* 29**,** 955-964.